


Article

Effects of Turbulence on the Vortex Modes Carried by Quasi-Diffracting Free Finite Energy Beam in Ocean

Qiyong Liang ¹, Yixin Zhang ^{1,2,*}  and Dongyu Yang ¹

¹ School of Science, Jiangnan University, Wuxi 214122, China; liangqiyong1006@126.com (Q.L.); 6181203003@stu.jiangnan.edu.cn (D.Y.)

² Jiangsu Provincial Research Center of Light Industrial Optoelectronic Engineering and Technology, Wuxi 214122, China

* Correspondence: zyx@jiangnan.edu.cn

Received: 26 May 2020; Accepted: 19 June 2020; Published: 22 June 2020



Abstract: By developing new wave structure function of a beam waves, we derive the transmitting probability of signal vortex modes in oceanic turbulence based on Rytov approximation theory. Applying this transmitting probability of signal vortex modes, we study the influence of oceanic turbulence on the transmittance of the vortex modes carried by Mathieu-Gaussian beam. This model shows the transmitting probability of Mathieu-Gaussian beam with narrow initial beam width, long wavelength, and small ellipticity parameter is higher than the transmitting probability of the signal vortex modes in case of the beam with wide initial beam width, short wavelength, and great ellipticity parameter. Furthermore, when Mathieu-Gaussian beam has a suitable semi-cone angle, the effect of weak-turbulence channel on the transmitting probability of signal vortex modes with different topological charge can be ignored. Mathieu-Gaussian beam is a more suitable carrier for high information channel of underwater wireless optical communication than Laguerre-Gaussian beam.

Keywords: oceanic turbulence; Mathieu-Gaussian beam; quasi-diffracting free finite energy beam; vortex topological charge; transmitting probability

1. Introduction

In recent years, underwater wireless optical communication have attracted a lot of attention due to the demands of underwater sensor networks, underwater unmanned devices, offshore exploration vessels and submarines [1–5]. However, turbulence in the seawater channel is an inevitable obstacle in the underwater wireless communication process, so it is necessary to reduce the signal attenuation and transmission capacity loss of the communication system caused by turbulence (diffraction) broadening of the beam [6–8]. To reduce the beam broadening caused by the beam edge diffraction and oceanic turbulence, quasi-diffracting free finite energy vortex beam become a new carrier of underwater wireless optical communication system. Because quasi-diffracting free finite energy vortex beam can be realized in experiments [9–14]. Because for that reason, there have been many reports on the performance of quasi-diffracting free finite energy vortex beam resist the beam expansion and channel capacity loss caused by oceanic turbulence [15–23]. Such as, the crosstalk probability of vortex modes of Lommel-Gaussian beam in anisotropic oceanic turbulence [15] and the beam wander of Lommel Gaussian-Schell beam in unstable stratification weak ocean-turbulence [16] were investigated. The capacity of a free space optical communication link with vortex modes carrier that is owned by Bessel-Gaussian beam in weak turbulent ocean [17] was explored, and the transmitting probability of vortex modes carried by Bessel-Gaussian localized wave in anisotropic turbulent ocean was derived by developing the spectrum average mutual coherence function of the Bessel-Gaussian localized wave and the spectrum average coherence length of spherical wave [18]. The results in [17] show that

Bessel-Gaussian beam has significant advantages over Laguerre-Gaussian beam in mitigating the effects of turbulence and enhancing the performance of the free-space optical communication link, as well as [18] show that Bessel-Gaussian localized wave is a more suitable beam for the vortex modes communication than conventional vortex beams. [19] indicates that the frozen wave has an optimal wavelength window in “seawater transmission window”. The transmitting probability of vortex modes of finite energy Airy vortex beam in anisotropic weak oceanic turbulence was analyzed [20]. The model shows that finite energy Airy beam having vortex topological charge larger than 5 is more resistant to turbulent disturbance than Laguerre-Gaussian beam [20]. Beam wander model of a partially coherent and finite energy Airy beam in weak to strong oceanic turbulence was derived [21]. The self-healing property of Bessel-Gaussian beam in an underwater environment was verified experimentally [22]. Besides, the performance of underwater optical communications based on optical vortices in the presence of water flow, stagnant water, air bubbles, and temperature difference was evaluated [23].

The non-diffracting beams have an infinite energy, thus they are difficult to realize in experiment. It is worth noting that the quasi-diffracting free beams of Lommel-Gaussian, Lommel Gaussian-Schell, Bessel-Gaussian, localized Bessel-Gaussian, and finite energy Airy solve the experimental generation dilemma of non-diffracting beams. However, due to the introduction of Gaussian truncation function [24], the ability of the Gaussian truncation non-diffracted beam to resist diffraction is greatly reduced. The Mathieu beam, which was introduced by Gutiérrez-Vega et al. [25], is a family of non-diffracting beams. Mathieu-Gaussian (MG) beam can be generated experimentally and is a very good approximation of non-diffracting Mathieu beam [26]. Therefore, this kind of beam should be the preferred one for underwater optical communication. That is, it is particularly necessary to study the anti-turbulence propagation performance of MG beam. However, to the best of our knowledge, the research for the propagation of MG beam in ocean turbulence was few reports.

In this paper, we investigated the propagation properties of signal vortex modes carried by MG beam in weak oceanic turbulence. To accurately describe the effect of ocean turbulence on this beam, in the study, we first studied and established the wave structure function of the beam wave. Then, we derived the expression of transmitting probability of the signal vortex modes for MG beam. By the transmitting probability of the signal vortex modes for MG beam, we discussed the influences of beam structure parameters and oceanic turbulence parameters on the transmitting probability of signal vortex modes in numerical calculation.

2. Wave Structure Function of Beam Waves

MG beam can be divided into four classes according to their even or odd modes [24,26,27], and the analytical expressions of four MG classes are similar in form. In this paper, for the sake of convenience, we consider $2l_0$ th-order even MG beam. By utilizing research conclusions in [27], the complex amplitude of the $2l_0$ th-order even MG beam propagation in turbulence-free communication link is expressed as

$$E_{2l_0}(r, \varphi, z) = \frac{1}{\sqrt{1+z_\xi^2}} \exp[ikz + i\frac{r^2}{w_0^2 z_\xi} - i \arctan(z_\xi)] \exp\left(-\frac{k_r^2 w_0^2 z_\xi}{4(z_\xi - i)} - \frac{r^2}{w_0^2 z_\xi (z_\xi - i)}\right) \times \sum_{p=0}^{\infty} A_{2p}^{(2l_0)}(q) (-1)^p \operatorname{Re}(e^{i2p\varphi}) J_{2p}\left(i\frac{k_r r}{z_\xi - i}\right), \quad (1)$$

where (r, φ, z) is the polar coordinates, $\operatorname{Re}(\cdot)$ indicates the real part, $i = \sqrt{-1}$, $z_\xi = 2z/kw_0^2$ is the non-dimensional coordinate, z is the propagation distance, $k = 2\pi/\lambda$ is the wavenumber with wavelength λ , w_0 is the initial beam width, $k_r = k \sin \beta$ is the transverse wavenumbers, β is the semi-angle of the conical wave that forms the MG beam, $2l_0$ is the vortex topological charge, p denote the number of sub-beams, q is the ellipticity parameter ($q = h^2 k_r^2 / 4$ and h is the interfocal parameter), $J_{2p}(\cdot)$ is the Bessel function of the first kind, $A_{2p}^{(2l_0)}(q)$ is an expansion coefficient of Mathieu functions, and the $A_{2p}^{(2l_0)}(q)$ can be obtained by using the recurrence equations between the expansion coefficient

of Mathieu functions (details are found in Ref. [28]). Particularly, when $2l_0 = 0$ and $q = 0$, MG beam degenerates into the zeroth-order Bessel-Gaussian beam.

Figure 1 depicts the transverse intensity distribution of a MG beam at $z = 0$ plane for different values of q and $2l_0$. Obviously, the MG beam morphology are determined by both q and $2l_0$. Similar to the zero-order Bessel Gaussian beam, zeroth-order MG beam present a circular symmetry when the parameter q tends to zero. And the MG beam morphology that is more complex and abundant than that of the Bessel-Gaussian beam.

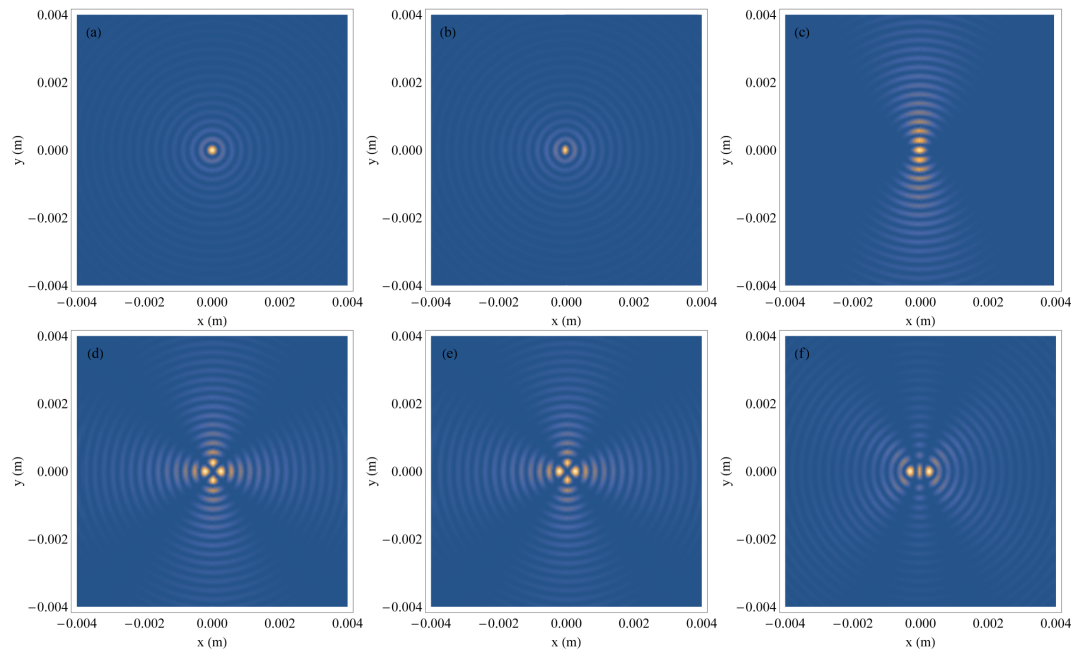


Figure 1. The transverse intensity pattern of Mathieu-Gaussian beam for (a) $2l_0 = 0, q = 0$, (b) $2l_0 = 0, q = 0.2$, (c) $2l_0 = 0, q = 5$, (d) $2l_0 = 2, q = 0$, (e) $2l_0 = 2, q = 0.2$, (f) $2l_0 = 2, q = 5$. The other beam parameters are $w_0 = 0.01$ m, $\lambda = 532$ nm, $\beta = 0.001$.

Rytov approximation is a good approximation to describe the law of light transmission in weakly turbulent media [29,30]. So, using the Rytov approximation, the complex amplitude $E_{2l_0}(r, \varphi, z)$ of MG beam propagating through weak oceanic turbulence at the receiver plane can be approximated as

$$E(r, \varphi, z) \approx E_{2l_0}(r, \varphi, z) \exp[\psi(r, \varphi, z)], \tag{2}$$

where $\psi(r, \varphi, z)$ is the random complex phase distortion caused by oceanic turbulence and $\psi(r, \varphi, z)$ satisfies [29]

$$\langle \exp[\psi(r, \varphi, z) + \psi^*(r', \varphi', z)] \rangle = \exp[-D_\psi(\mathbf{r}, \mathbf{r}', z)/2] = \exp\left(-\frac{|\mathbf{r} - \mathbf{r}'|^2}{\rho_{oc}^2}\right), \tag{3}$$

where $\langle \cdot \rangle$ denotes the ensemble average of oceanic turbulence, $D_\psi(\mathbf{r}, \mathbf{r}', z)$ is the wave structure function, and ρ_{oc} is the spatial coherence radius of beam waves propagating in oceanic turbulence.

Mathematically, MG beam is an infinite sum of Bessel-Gaussian beam of various orders, and the Bessel-Gaussian beam is a kind of beam formed by truncating plane waves with Gaussian aperture. Therefore, to accurately describe the effect of ocean turbulence on MG beam, the $D_\psi(\mathbf{r}, \mathbf{r}', z)$ in Equation (3) should be calculated by the wave structure function of the beam wave.

Suppose that light propagates in oceanic turbulence along horizontal path, so that the wave structure function is expressed in the form [29]

$$D_\psi(\mathbf{r}, \mathbf{r}', z) = 8\pi^2 k^2 z \int_0^1 \int_0^\infty \kappa \Phi(\kappa) \exp(-\Lambda z \kappa^2 \xi^2 / k) \times \{1 - J_0[\kappa |(1 - \bar{\Theta}\xi)(\mathbf{r} - \mathbf{r}') - i\Lambda\xi(\mathbf{r} + \mathbf{r}')|]\} dk d\xi \quad (4)$$

here $\Lambda = \frac{2z}{kw^2(z)}$, $w(z) = w_0 \sqrt{(1 - z/F_0)^2 + \frac{4z^2}{k^2 w_0^4}}$, and $\bar{\Theta} = 1 - \frac{(F_0 - z)kw_0^2}{F_0 kw^2(z)}$, $\Phi(\kappa)$ and κ represent the power spectrum of refractive-index fluctuations and the spatial frequency respectively.

In general, the integral of Equation (4) cannot be calculated. But, in the case of the forward scattering approximation (or the near-axial transmission approximation), the zeroth-order Bessel function can be approximated as the first two terms of the expanded series

$$J_0[\kappa |(1 - \bar{\Theta}\xi)(\mathbf{r}_1 - \mathbf{r}_2) - i\Lambda\xi(\mathbf{r}_1 + \mathbf{r}_2)|] \approx 1 - \frac{\kappa^2}{4} [(1 - \bar{\Theta}\xi)^2 |\mathbf{r}_1 - \mathbf{r}_2|^2 - i\Lambda\xi(1 - \bar{\Theta}\xi)(\mathbf{r}_1^2 - \mathbf{r}_2^2) - \Lambda^2 \xi^2 |\mathbf{r}_1 + \mathbf{r}_2|^2] \quad (5)$$

When $|\mathbf{r}| = |\mathbf{r}'| = r$, make use of the relation $|\mathbf{r} - \mathbf{r}'|^2 = 2r^2(1 - \cos(\varphi - \varphi'))$, $|\mathbf{r} + \mathbf{r}'|^2 = 2r^2(1 + \cos(\varphi - \varphi'))$, $\mathbf{r}^2 - \mathbf{r}'^2 = 0$. The Equation (5) is simplified as follows:

$$D_\psi(\mathbf{r}, \mathbf{r}, z) = 2\pi^2 k^2 z \int_0^\infty \kappa^3 \Phi(\kappa) \left\{ \int_0^1 [(1 - 2\bar{\Theta}\xi + \bar{\Theta}^2 \xi^2) [2r^2(1 - \cos(\varphi - \varphi'))] - \Lambda^2 \xi^2 [2r^2(1 + \cos(\varphi - \varphi'))]] \exp(-\Lambda z \kappa^2 \xi^2 / k) d\xi \right\} d\kappa \quad (6)$$

Now we have the definite integral relations [31] $\int_0^1 \xi^m \exp(-\beta\xi^n) d\xi = -\frac{\Gamma(\frac{m+1}{n}, \beta)}{(n\beta^{\frac{m+1}{n}})} + \frac{\Gamma(\frac{m+1}{n}, 0)}{(n\beta^{\frac{m+1}{n}})}$

and $\int_0^1 e^{-\beta\xi^2} d\xi = \frac{1}{2} \sqrt{\pi/\beta} e^{\beta} - \frac{1}{2} \sqrt{\pi/\beta}$. Equation (6) therefore reduces to

$$D_\psi(\mathbf{r}, \mathbf{r}, z) = 2\pi^2 k^2 z \int_0^\infty \kappa^3 \Phi(\kappa) \left\{ \frac{1}{2\kappa} \sqrt{\frac{\pi k}{\Lambda z}} (e^{\kappa\sqrt{\Lambda z/k}} - 1) [2r^2(1 - \cos(\varphi - \varphi'))] - \bar{\Theta} \frac{\Gamma(1,0) - \Gamma(1, \Lambda z \kappa^2 / k)}{\Lambda z \kappa^2 / k} [2r^2(1 - \cos(\varphi - \varphi'))] + \bar{\Theta}^2 \frac{\Gamma(3/2,0) - \Gamma(3/2, \Lambda z \kappa^2 / k)}{2(\Lambda z \kappa^2 / k)^{3/2}} \times [2r^2(1 - \cos(\varphi - \varphi'))] - \Lambda^2 [2r^2(1 + \cos(\varphi - \varphi'))] \frac{\Gamma(3/2,0) - \Gamma(3/2, \Lambda z \kappa^2 / k)}{2(\Lambda z \kappa^2 / k)^{3/2}} \right\} d\kappa \quad (7)$$

Consider Gaussian beams ($F_0 = \infty$) and 300 m long underwater optical communication link, we have following approximations $\Lambda \approx \frac{2z}{kw_0^2}$, $\Lambda^2 \approx 0$, $e^{\kappa\sqrt{\Lambda z/k}} - 1 \approx \kappa\sqrt{\Lambda z/k}$, $\bar{\Theta} \approx 0$.

Now, Equation (7) simplifies as

$$D_\psi(\mathbf{r}, \mathbf{r}, z) = 2\sqrt{\pi} \pi^2 z k^2 r^2 [1 - \cos(\varphi - \varphi')] \int_0^\infty \kappa^3 \Phi(\kappa) d\kappa \quad (8)$$

On substituting Equation (8) into Equation (3), the spatial coherence radius of beam waves ρ_{oc} can be expressed as

$$\rho_{oc} = \left[(\sqrt{\pi}/2) \pi^2 k^2 z \int_0^\infty \kappa^3 \Phi(\kappa) d\kappa \right]^{-1/2} \quad (9)$$

As for an-isotropic oceanic turbulence, the power spectrum of refractive-index fluctuations is given by [32–34]

$$\Phi(\kappa) = 0.388 \times 10^{-8} \chi_t \varepsilon^{-1/3} \zeta^2 \kappa^{-11/3} [1 + 2.35(\kappa\eta)^{2/3}] f(\kappa, \omega) \quad (10)$$

where $\kappa = \sqrt{\kappa_x^2 + \zeta^2 \kappa_\rho^2}$ is the spatial frequency of the refractive index fluctuations, $\kappa_\rho = \sqrt{\kappa_x^2 + \kappa_y^2}$, under the Markov approximation, κ can be further simplified as $\kappa = \zeta \kappa_\rho$, ζ is the an-isotropic

factor of turbulence, ω is the contribution ratio of temperature and salinity fluctuations for turbulent ocean, ε is the dissipation rate of kinetic energy per unit mass of fluid, χ_t is the dissipation rate of the mean-squared temperature, η is the inner scale of turbulence, $f(\kappa, \omega) = [\exp(-A_T\delta) + \omega^{-2} \exp(-A_S\delta) - 2\omega^{-1} \exp(-A_{TS}\delta)]$, $A_T = 1.863 \times 10^{-2}$, $A_S = 1.9 \times 10^{-4}$, $A_{TS} = 9.41 \times 10^{-3}$, $\delta = 8.284(\kappa\eta)^{4/3} + 12.978(\kappa\eta)^2$.

On substituting Equation (10) into Equation (9), after a long but straightforward calculation [35], the spatial coherence radius of beam waves in oceanic turbulence is given by

$$\rho_{oc} = \left[3 \times 10^{-8} k^2 \pi^2 (\sqrt{\pi}/2) z \chi_t \zeta^{-2} \omega^{-2} (\varepsilon \eta)^{-1/3} (0.876\omega^2 - 2.247\omega + 6.128) \right]^{-1/2}. \quad (11)$$

3. Transmitting Probability of Signal Vortex Modes

As discussed in literature [36,37], the complex amplitude $E(r, \varphi, z)$ of MG beam can be decomposed into a superposition of several vortex modes

$$E(r, \varphi, z) = \frac{1}{\sqrt{2\pi}} \sum_{l=-\infty}^{\infty} \beta_l \exp(il\varphi), \quad (12)$$

where β_l is expansion coefficient, the ensemble average $\langle |\beta_l|^2 \rangle$ represents the probability density of vortex modes in oceanic turbulence, which has the form of

$$\langle |\beta_l|^2 \rangle = \frac{1}{2\pi} \int_0^{2\pi} \int_0^{2\pi} E(r, \varphi, z) E^*(r, \varphi, z) \exp[-il(\varphi - \varphi')] d\varphi d\varphi'. \quad (13)$$

By combining Equation (1) with Equation (2) and Equation (13), probability density $\langle |\beta_l|^2 \rangle$ of vortex modes of the MG beam is calculated as

$$\begin{aligned} \langle |\beta_l|^2 \rangle &= \frac{(2\pi)^{-1}}{1+z_\zeta^2} \exp\left[-\frac{k_r^2 w_0^2 z_\zeta^2}{2(z_\zeta^2+1)}\right] \exp\left[-\frac{2r^2}{w_0^2(z_\zeta^2+1)}\right] \\ &\times \exp\left[-\frac{2r^2}{\rho_{oc}^2}\right] \sum_{p=0}^{\infty} \sum_{p'=0}^{\infty} A_{2p}^{(2l_0)}(q) A_{2p'}^{(2l_0)}(q) (-1)^{p+p'} \\ &\times J_{2p}\left(i\frac{kr}{z_\zeta-i}\right) J_{2p'}^*\left(i\frac{kr}{z_\zeta-i}\right) \int_0^{2\pi} \int_0^{2\pi} d\varphi d\varphi' \exp\left[\frac{2r^2 \cos(\varphi-\varphi')}{\rho_{oc}^2}\right] \\ &\times \text{Re}\{\exp[i(2p\varphi - 2p'\varphi')]\} \exp[-il(\varphi - \varphi')] \end{aligned} \quad (14)$$

With the help of the integral expression [31]

$$\int_0^{2\pi} \exp[\vartheta \cos(\theta - \phi) - im\theta] d\theta = 2\pi \exp(-im\phi) I_m(\vartheta), \quad (15)$$

where $I_m(\cdot)$ denotes the symbol of the modified Bessel function of the first kind, the probability density $\langle |\beta_l|^2 \rangle$ of vortex modes of the MG beam is given by

$$\begin{aligned} \langle |\beta_l|^2 \rangle &= \frac{2\pi}{1+z_\zeta^2} \exp\left[-\frac{k_r^2 w_0^2 z_\zeta^2}{2(z_\zeta^2+1)}\right] \exp\left[-2\left(\frac{1}{w_0^2(z_\zeta^2+1)} + \frac{1}{\rho_{oc}^2}\right)r^2\right] \\ &\times \sum_{p=0}^{\infty} \left[A_{2p}^{(2l_0)}(q)\right]^2 \left|J_{2p}\left(i\frac{kr}{z_\zeta-i}\right)\right|^2 \text{Re}\left[I_{l-2p}\left(\frac{2r^2}{\rho_{oc}^2}\right)\right] \end{aligned} \quad (16)$$

Considering a receiver with an aperture diameter of D , we obtain the energy for each received vortex modes of the MG beam

$$M_l = \frac{2\pi}{1+z\zeta} \exp\left[-\frac{k_r^2 w_0^2 z^2 \zeta}{2(z\zeta+1)}\right] \sum_{p=0}^{\infty} [A_{2p}^{(2l_0)}(q)]^2 \int_0^{D/2} dr \times \exp\left[-2\left(\frac{1}{w_0^2(z\zeta+1)} + \frac{1}{\rho_{oc}^2}\right)r^2\right] |J_{2p}\left(i\frac{k_r r}{z\zeta-i}\right)|^2 \operatorname{Re}\left[I_{l-2p}\left(\frac{2r^2}{\rho_{oc}^2}\right)\right] r \quad (17)$$

Then we define the normalized energy for each received vortex modes of the MG beam as follows:

$$P_l = M_l / \sum_{l'=-\infty}^{\infty} M_{l'} \quad (18)$$

where P_l can be regarded as the normalized transmitting probability of signal vortex modes of the MG beam when $l - 2l_0 = 0$. P_l can be regarded as the normalized crosstalk probability of vortex modes of the MG beam when $l - 2l_0 \neq 0$, $\sum_{l'=-\infty}^{\infty} M_{l'}$ denotes the total received energy.

4. Effects of the Parameters of Oceanic Turbulence and Mathieu-Gaussian Beam

To explore the influence of beam structure parameters and oceanic turbulence parameters on the transmission of vortex modes, in this section, we numerically study the transmitting probability of signal vortex modes for a MG beam propagating in an anisotropic oceanic turbulence. In the following analysis, we set the calculation parameters as: $q = 0.2$, $2l_0 = 2$, $l = 2$, $w_0 = 0.05$ m, $D = 0.1$ m, $\beta = 0.0001$, $z = 150$ m, $\lambda = 561$ nm, $\chi_t = 10^{-8}$ K²/s, $\varepsilon = 10^{-5}$ m²/s³, $\eta = 1$ mm, $\omega = -4.5$, and $\zeta = 2$, unless other variable parameters are specified in calculation. In this section, we first analyze the influence of system parameters on the transmission of signal vortex modes, and then analyze the influence of oceanic turbulence on them.

4.1. Influence of System Parameters

Figure 2 reveals that the energy of the emitted vortex modes spreads into the adjacent vortex modes for different values of the vortex topological charge $2l_0$ and the semi-cone angle β . Comparatively speaking, the transmitting probability of signal vortex modes of the MG beam decreases and modes crosstalk becomes more significant as β increases. When $\beta = 0.0002$ and $\beta = 0.0003$, the effect of weak-turbulence channel on the transmitting probability of signal vortex mode with different vortex topological charge can be ignored. When $\beta = 0.0001$, the magnitude of the transmitting probability of signal vortex modes decreases with increase of the vortex topological charge $2l_0$. Theoretically, we can improve the information capacity of the communication channel by selecting a suitable semi-cone angle and using the high-order vortex modes of the beam as the information carrier.

Figure 3 shows the dependence of the transmitting probability of signal vortex modes of the MG beam on initial beam width w_0 , received diameter D and propagation distance z . As would be expected, the magnitude of the transmitting probability of signal vortex modes decreases with increase of the propagation distance z . In Figure 3a, the value of the transmitting probability of signal vortex modes decreases with increase of the w_0 . The reason for this result is that as the increase of the beam diameter, the number of turbulent eddies that have different refractive indexes in the beam also increases, which increases the wavefront aberration of the beam. As a consequence, a larger w_0 leads to lower transmitting probability of signal vortex modes. As shown as in Figure 3b, when D increases, the value of the transmitting probability of signal vortex modes decreases first and then reaches a steady state. The phenomenon could be explained that the wave front aberration increases as increase of the D , which cause larger inter-mode crosstalk of vortex modes [18]. As a consequence,

the aperture receiver with larger D leads to the transmitting probability decreases. When the receiver aperture diameter is large enough, the whole beam spot is fully received, the transmitting probability of signal vortex modes is no longer dependent on D .

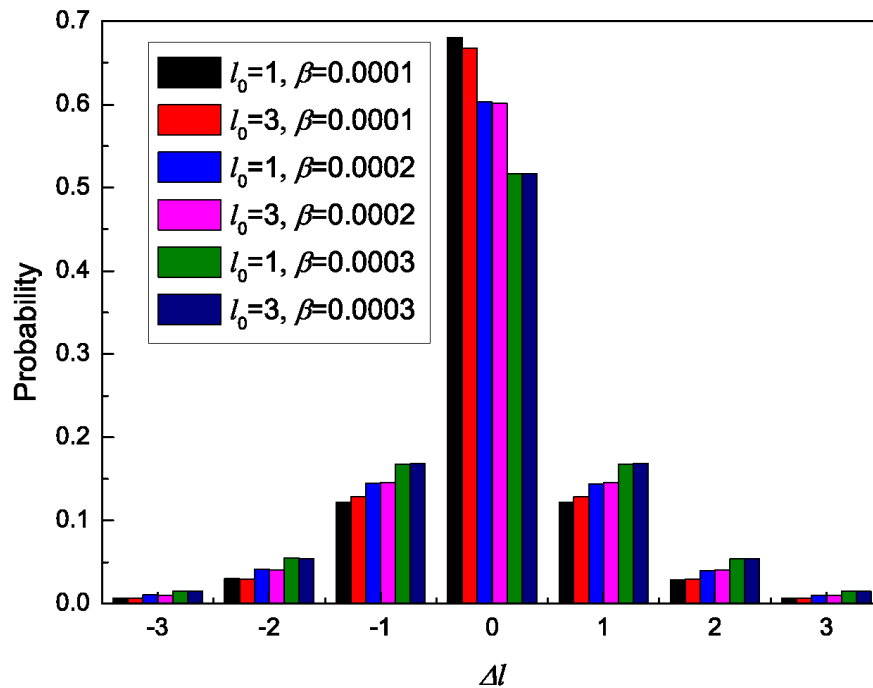


Figure 2. The normalized energy for each received vortex modes carried by Mathieu-Gaussian beam propagating in oceanic turbulence for different values of vortex topological charge $2l_0$ and semi-cone angle β ($\Delta l = l - 2l_0$).

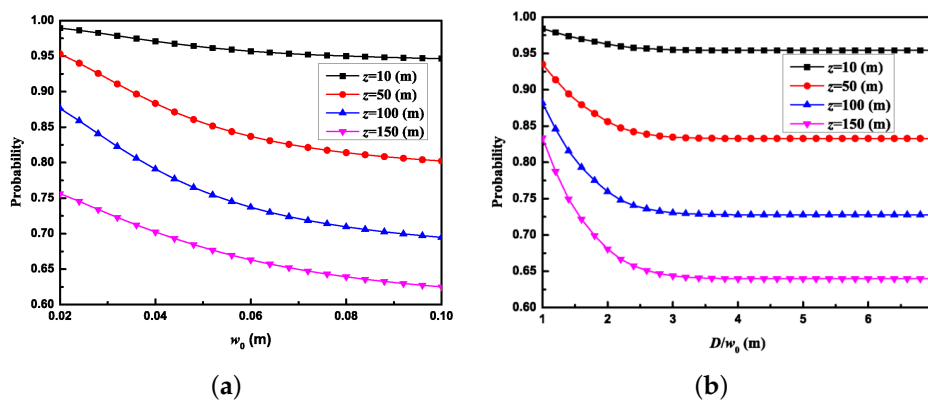


Figure 3. The normalized transmitting probability of the signal vortex modes versus (a) initial beam width w_0 and (b) received diameter D with $w_0 = 0.05$ m for different values of propagation distance z .

Figure 4 illustrates the impact of the wavelength λ on the transmitting probability of signal vortex modes of the MG beam with different values of ellipticity parameter q . We find that the value of the transmitting probability of signal vortex modes decreases as q increases. It means that the MG beam with small ellipticity parameter is more suitable for underwater wireless optical communication. Like any other type of beam, the transmitting probability of signal vortex modes decreases with decreasing λ . This is because the long-wavelength beam has lower scintillation [29].

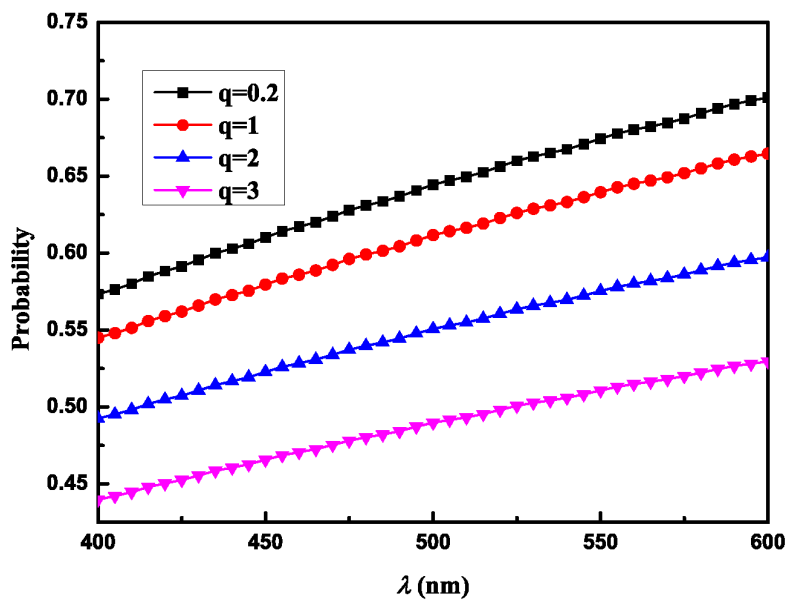


Figure 4. The normalized transmitting probability of the signal vortex modes versus wavelength λ for different values of ellipticity parameter q .

4.2. Influence of Oceanic Turbulence

To comprehend the effects of turbulence parameters on the transmitting probability of signal vortex modes of the MG beam, we investigate the effects of the dissipation rate of kinetic energy per unit mass of fluid ε and the inner scale of turbulence η on the transmitting probability of signal vortex modes of the MG beam. From Figure 5, one can see that the value of the transmitting probability of signal vortex modes increases with increase of the ε and η , as expected [5,8,34]. The former is because the strength of oceanic turbulence decreases with the increasing of ε . The latter is because a larger η corresponding to a weaker scattering.

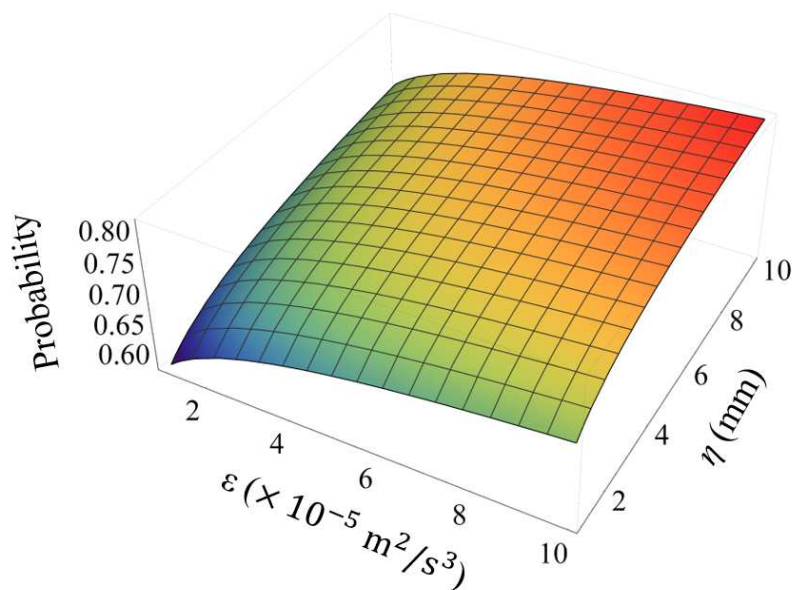


Figure 5. The normalized transmitting probability of the signal vortex modes versus dissipation rate of kinetic energy per unit mass of fluid ε and inner scale of turbulence η .

In Figure 6, we investigate the effects of the temperature-salinity contribution ratios ω , dissipation rate of the mean-squared temperature χ_t and an-isotropic factor of turbulence ζ on the transmitting probability of signal vortex modes of the MG beam. When ζ equals 1, the an-isotropic oceanic turbulence can degrade into the isotropic oceanic turbulence. It is clear from the Figure 6 that the magnitude of the transmitting probability of signal vortex modes decreases with increasing ω , and χ_t , as well as, decreasing ζ . This result also is consistent with the result in Ref. [5,8,34].

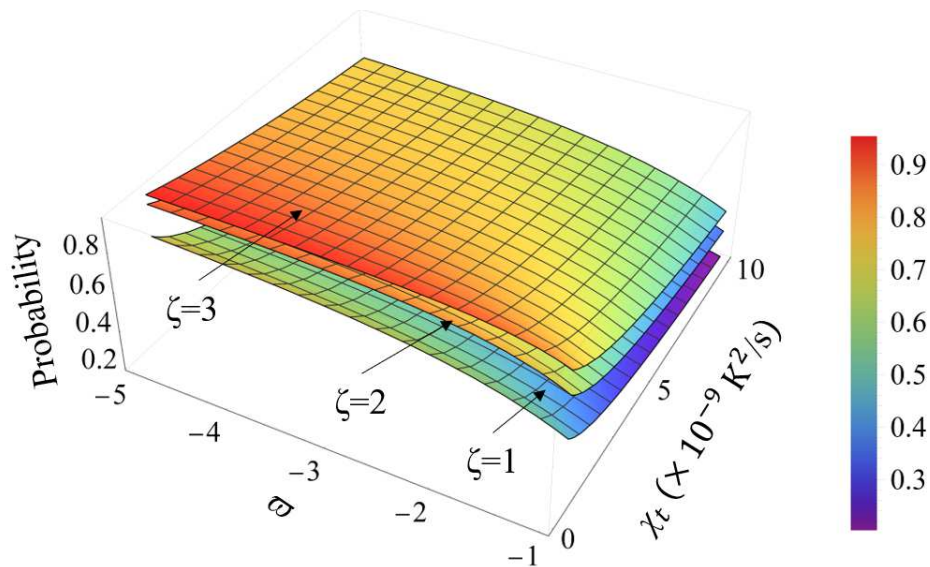


Figure 6. The normalized transmitting probability of the signal OAM modes versus temperature-salinity contribution ratios ω , dissipation rate of the mean-squared temperature χ_t and an-isotropic factor of turbulence ζ .

5. Summary

In summary, we focused on the propagation properties of vortex modes carried by the MG beam in an-isotropic oceanic turbulence and developed the wave structure function of beam waves, as well as, we derived the transmitting probability of signal vortex modes of the MG beam. The MG beam with small initial beam width, long wavelength, and small ellipticity parameter has larger ability to obstruct turbulence disturbance. Also, our results reveal that, theoretically, we can improve the information capacity of the communication channel by selecting a suitable semi-cone angle and using the high-order vortex modes of the beam as the information carrier. This result indicates that the MG beam is a beam that is more suitable as the source of the optical communication system than the Laguerre-Gaussian beam [7,8,38], because the higher topological charge of the vortex modes carried by the Laguerre-Gaussian beam, the lower the transmittance. In addition, the effect of turbulence on the transmission pattern of vortex carried by MG beam is consistent with that of vortex modes carried by conventional beam, namely: the signal vortex modes carried by MG beam suffers less turbulence disturbance in oceanic turbulence with lower dissipation rate of the mean-squared temperature, larger an-isotropic factor, smaller temperature-salinity contribution ratios, larger inner scale, and higher dissipation rate of kinetic energy per unit mass of fluid. Furthermore, a small-aperture receiver is beneficial to enhancing transmitting probability of the signal vortex modes.

Author Contributions: Conceptualization, Y.Z.; methodology, software and writing-review & editing, Q.L.; formal analysis, Y.Z.; validation, D.Y. All authors have read and agreed to the published version of the manuscript.

Funding: This work was supported by the National Natural Science Foundation of China [Grant No. 61871202] and the Postgraduate Research & Practice Innovation Program of Jiangsu Province [Grant No. 1142050205206114].

Conflicts of Interest: The authors declare no conflict of interest.

References

1. Cui, X.; Yin, X.; Chang, H.; Guo, Y.; Zheng, Z.; Sun, Z.; Liu, G.; Wang, Y. Analysis of an adaptive orbital angular momentum shift keying decoder based on machine learning under oceanic turbulence channels. *Opt. Commun.* **2018**, *429*, 138–143. [[CrossRef](#)]
2. Baykal, Y.; Ata, Y.; Gökçe, M.C. Structure parameter of anisotropic atmospheric turbulence expressed in terms of anisotropic factors and oceanic turbulence parameters. *Appl. Opt.* **2019**, *2*, 454–460. [[CrossRef](#)] [[PubMed](#)]
3. Luo, B.; Wu, G.; Yin, L.; Gui, Z.; Tian, Y. Propagation of optical coherence lattices in oceanic turbulence. *Opt. Commun.* **2018**, *425*, 80–84. [[CrossRef](#)]
4. Ata, Y.; Baykal, Y. Effect of anisotropy on bit error rate for an asymmetrical Gaussian beam in a turbulent ocean. *Appl. Opt.* **2018**, *57*, 2258–2262. [[CrossRef](#)] [[PubMed](#)]
5. Yi, X.; Djordjevic, I.B. Power spectrum of refractive-index fluctuations in turbulent ocean and its effect on optical scintillation. *Opt. Express* **2018**, *26*, 10188–10202. [[CrossRef](#)]
6. Pan, S.; Wang, L.; Wang, W.; Zhao, S. An Effective Way for Simulating Oceanic Turbulence Channel on the Beam Carrying Orbital Angular Momentum. *Sci. Rep.* **2019**, *9*, 14009. [[CrossRef](#)]
7. Li, Y.; Cui, Z.; Han, Y.; Hui, Y. Channel capacity of orbital-angular-momentum based wireless communication systems with partially coherent elegant Laguerre-Gaussian beams in oceanic turbulence. *J. Opt. Soc. Am. A* **2019**, *36*, 471–477. [[CrossRef](#)] [[PubMed](#)]
8. Yi, X.; Zheng, R.; Yue, P.; Ding, W.; Shen, C. Propagation properties of OAM modes carried by partially coherent LG beams in turbulent ocean based on an oceanic power-law spectrum. *Opt. Commun.* **2019**, *443*, 238–244. [[CrossRef](#)]
9. Siviloglou, G.A.; Broky, J.; Dogariu, A.; Christodoulides, D.N. Observation of accelerating Airy beams. *Phys. Rev. Lett.* **2007**, *99*, 213901. [[CrossRef](#)] [[PubMed](#)]
10. Chu, X.; Sun, Q.; Wang, J.; Lu, P.; Xie, W.; Xu, X. Generating a Bessel-Gaussian beam for the application in optical engineering. *Sci. Rep.* **2016**, *5*, 18665. [[CrossRef](#)]
11. López-Mariscal, C.; Bandres, M.A.; Gutiérrez-Vega, J.C. Observation of the experimental propagation properties of Helmholtz-Gauss beams. *Opt. Eng.* **2006**, *45*, 068001. [[CrossRef](#)]
12. Alvarez-Elizondo, M.B.; Rodríguez-Masegosa, R.; Gutiérrez-Vega, J.C. Generation of Mathieu-Gauss modes with an axicon-based laser resonator. *Opt. Express* **2008**, *16*, 18770–18775. [[CrossRef](#)]
13. Zhao, Q.; Gong, L.; Li, Y. Shaping diffraction-free Lommel beams with digital binary amplitude masks. *Appl. Opt.* **2015**, *54*, 7553–7558. [[CrossRef](#)]
14. Zamboni-Rached, M.; Mojahedi, M. Shaping finite-energy diffraction- and attenuation-resistant beams through Bessel-Gauss beam superposition. *Phys. Rev. A* **2015**, *92*, 043839. [[CrossRef](#)]
15. Yu, L.; Zhang, Y. Analysis of modal crosstalk for communication in turbulent ocean using Lommel-Gaussian beam. *Opt. Express* **2017**, *25*, 22565–22574. [[CrossRef](#)]
16. Liang, Q.; Zhu, Y.; Zhang, Y. Approximations wander model for the Lommel Gaussian-Schell beam through unstable stratification and weak ocean-turbulence. *Results Phys.* **2019**, *14*, 102511. [[CrossRef](#)]
17. Cheng, M.; Guo, L.; Li, J.; Zhang, Y. Channel Capacity of the OAM-Based Free-Space Optical Communication Links With Bessel-Gauss Beams in Turbulent Ocean. *IEEE Photonics J.* **2016**, *8*, 1–11. [[CrossRef](#)]
18. Deng, S.; Zhu, Y.; Zhang, Y. Received Probability of Vortex Modes Carried by Localized Wave of Bessel-Gaussian Amplitude Envelope in Turbulent Seawater. *J. Mar. Sci. Eng.* **2019**, *7*, 203. [[CrossRef](#)]
19. Deng, S.; Yang, D.; Zheng, Y.; Hu, L.; Zhang, Y.; Transmittance of finite-energy frozen beams in oceanic turbulence. *Results Phys.* **2019**, *15*, 102802. [[CrossRef](#)]
20. Wang, X.; Yang, Z.; Zhao, S. Influence of oceanic turbulence on propagation of Airy vortex beam carrying orbital angular momentum. *Optik* **2019**, *176*, 49–55. [[CrossRef](#)]
21. Jin, Y.; Hu, M.; Luo, M.; Luo, Y.; Mi, X.; Zou, C.; Shu, C.; Zhu, X.; He, J.; Ouyang, S.; et al. Beam wander of a partially coherent Airy beam in oceanic turbulence. *J. Opt. Soc. Am. A* **2018**, *35*, 1457–1464. [[CrossRef](#)]
22. Zhao, S.; Zhang, W.; Wang, L.; Li, W.; Gong, L.; Cheng, W.; Chen, H.; Gruska, J. Propagation and self-healing properties of Bessel-Gaussian beam carrying orbital angular momentum in an underwater environment. *Sci. Rep.* **2019**, *9*, 2025. [[CrossRef](#)]

23. Karahroudi, M.K.; Moosavi, S.A.; Mobashery, A.; Parmoon, B.; Saghafifar, H. Performance evaluation of perfect optical vortices transmission in an underwater optical communication system. *Appl. Opt.* **2018**, *57*, 9148–9154. [[CrossRef](#)]
24. Chafiq, A.; Hricha, Z.; Belafhal, A. A detailed study of Mathieu-Gauss beams propagation through an apertured ABCD optical system. *Opt. Commun.* **2006**, *265*, 594–602. [[CrossRef](#)]
25. Gutiérrez-Vega, J.C.; Iturbe-Castillo, M.D.; Chávez-Cerda, S. Alternative formulation for invariant optical fields: Mathieu beams. *Opt. Lett.* **2000**, *25*, 1493–1495. [[CrossRef](#)]
26. Chafiq, A.; Hricha, Z.; Belafhal, A. Propagation of generalized Mathieu-Gauss beams through paraxial misaligned optical systems. *Opt. Commun.* **2009**, *282*, 3934–3939. [[CrossRef](#)]
27. Chafiq, A.; Hricha, Z.; Belafhal, A. Paraxial propagation of Mathieu beams through an apertured ABCD optical system. *Opt. Commun.* **2005**, *253*, 223–230. [[CrossRef](#)]
28. Eyyuboğlu, H.T. A study of source plane Mathieu beams. *Appl. Phys. B* **2008**, *91*, 629–637. [[CrossRef](#)]
29. Andrews, L.C.; Phillips, R.L. *Laser Beam Propagation Through Random Media*; SPIE Press: Washington, DC, USA, 2005.
30. Korotkova, O. Light Propagation in a Turbulent Ocean. *Prog. Opt.* **2018**, *64*, 1–43.
31. Gradshteyn, I.S.; Ryzhik, I.M.R. *Tables of Integrals, Series, and Products*, 5th ed.; Academic Press: New York, NY, USA, 1994.
32. Nikishov, V.V.; Nikishov, V.I. Spectrum of turbulent fluctuations of the sea-water refraction index. *Int. J. Fluid Mech. Res.* **2000**, *27*, 82–98. [[CrossRef](#)]
33. Baykal, Y. Effect of anisotropy on intensity fluctuations in oceanic turbulence. *J. Mod. Opt.* **2018**, *65*, 825–829. [[CrossRef](#)]
34. Li, Y.; Yu, L.; Zhang, Y. Influence of anisotropic turbulence on the orbital angular momentum modes of Hermite-Gaussian vortex beam in the ocean. *Opt. Express* **2017**, *25*, 12203–12215. [[CrossRef](#)] [[PubMed](#)]
35. Yang, Y.; Yu, L.; Wang, Q.; Zhang, Y. Wander of the short-term spreading filter for partially coherent Gaussian beams through the anisotropic turbulent ocean. *Appl. Opt.* **2017**, *56*, 7046–7052. [[CrossRef](#)] [[PubMed](#)]
36. Paterson, C. Atmospheric turbulence and orbital angular momentum of single photons for optical communication. *Phys. Rev. Lett.* **2005**, *94*, 153901. [[CrossRef](#)]
37. Yang, J.; Zhang, H.; Zhang, X.; Li, H.; Xi, L. Transmission Characteristics of Adaptive Compensation for Joint Atmospheric Turbulence Effects on the OAM-Based Wireless Communication System. *Appl. Sci.* **2019**, *9*, 901. [[CrossRef](#)]
38. Li, Y.; Han, Y.; Cui, Z.; Hui, Y. Performance analysis of the OAM based optical wireless communication systems with partially coherent elegant Laguerre-Gaussian beams in oceanic turbulence. *J. Opt.* **2019**, *21*, 035702. [[CrossRef](#)]

